

activity and diversity of particle-emitting organisms seem likely to play important roles in Earth history and future global change.

References and Notes

- J. L. Jimenez *et al.*, *Science* **326**, 1525 (2009).
- M. Hallquist *et al.*, *Atmos. Chem. Phys.* **9**, 5155 (2009).
- S. Solomon, *IPCC 4th Assessment Report* (Cambridge Univ. Press, Cambridge, 2007).
- M. O. Andreae, *Science* **315**, 50 (2007).
- S. T. Martin *et al.*, *Rev. Geophys.* **48**, RG2002 (2010).
- U. Pöschl *et al.*, *Science* **329**, 1513 (2010).
- Q. Chen *et al.*, *Geophys. Res. Lett.* **36**, L20806 (2009).
- D. V. Spracklen *et al.*, *Atmos. Chem. Phys.* **6**, 5631 (2006).
- R. Weigel *et al.*, *Atmos. Chem. Phys.* **11**, 9983 (2011).
- A. M. L. Ekman *et al.*, *Geophys. Res. Lett.* **35**, L17810 (2008).
- Materials and methods are available as supplementary materials on Science Online.
- A. V. Tivanski, R. J. Hopkins, T. Tyliczszak, M. K. Gilles, *J. Phys. Chem. A* **111**, 5448 (2007).
- S. F. Maria, L. M. Russell, M. K. Gilles, S. C. B. Myneni, *Science* **306**, 1921 (2004).
- M. Claeys *et al.*, *Science* **303**, 1173 (2004).
- J. L. Goatley, R. W. Lewis, *Plant Physiol.* **41**, 373 (1966).
- W. Elbert, P. E. Taylor, M. O. Andreae, U. Pöschl, *Atmos. Chem. Phys.* **7**, 4569 (2007).
- M. O. Andreae, *Science* **220**, 1148 (1983).
- J. Li, M. Posfai, P. V. Hobbs, P. R. Buseck, *J. Geophys. Res.* **108**, 8484 (2003).
- http://sigma.cptec.inpe.br/queimadas/v_anterior/dados_ant/dp_anteriores.html.
- <http://firefly.geog.umd.edu/firemap> [accessed 23 March 2012].
- P. Artaxo, H. C. Hansson, *Atmos. Environ.* **29**, 393 (1995).
- M. O. Andreae, P. J. Crutzen, *Science* **276**, 1052 (1997).
- P. Artaxo, W. Maenhaut, H. Storms, R. Vangrieken, *J. Geophys. Res.* **95**, 16971 (1990).
- A. Worobiec *et al.*, *Atmos. Environ.* **41**, 9217 (2007).
- D. R. Lawson, J. W. Winchester, *J. Geophys. Res.* **84**, 3723 (1979).
- D. R. Lawson, J. W. Winchester, *Geophys. Res. Lett.* **5**, 195 (1978).
- G. E. Nemeryuk, *Sov. Plant Physiol.* **17**, 560 (1970).
- G. Crozat, *Tellus* **31**, 52 (1979).
- W. Beauford, J. Barber, A. R. Barringer, *Science* **195**, 571 (1977).
- W. Beauford, J. Barber, A. R. Barringer, *Nature* **256**, 35 (1975).
- A. K. Bertram *et al.*, *Atmos. Chem. Phys.* **11**, 10995 (2011).
- M. Song, C. Marcolli, U. K. Krieger, A. Zuend, T. Peter, *Atmos. Chem. Phys.* **12**, 2691 (2012).
- A. Zuend, J. H. Seinfeld, *Atmos. Chem. Phys.* **12**, 3857 (2012).
- S. S. Gunthe *et al.*, *Atmos. Chem. Phys.* **9**, 7551 (2009).

Acknowledgments: This work has been supported by the Max Planck Society, the Max Planck Graduate Center, the Geocycles Cluster Mainz (Landesexzellenzcluster Rheinland-Pfalz),

and the European Community (PEGASOS, FP7-265148). The Harvard Environmental Chamber was supported by the Office of Science, Office of Basic Energy Sciences (BES), U.S. Department of Energy (DOE), grant no. DE-FG02-08ER6452, and the U.S. NSF under grant no. 0925467. The Advanced Light Source is supported by the Director, Office of Science, BES, of the U.S. DOE under contract no. DE-AC02-05CH11231. We thank the Helmholtz-Zentrum Berlin for the allocation of synchrotron radiation beamtime at BESSY II. We thank the Instituto Nacional de Pesquisas da Amazônia (INPA), Manaus, and the ATTO team under the Brazilian coordinator, A. O. Manzi, for their collaboration and field support. We also thank G. R. Carmichael and the Center for Global and Regional Environmental Research at the University of Iowa for support in the Weather Research and Forecasting (WRF) model simulations. We gratefully acknowledge R. Ditz, I. Trebs, X. Chi, J. A. Huffman, J. Kesselmeier, J. Schöngart, M. Kuwata, T. Tyliczszak, J. Huth, G. Schütz, E. Goering, M. Bechtel, J.-D. Förster, and T. Behrendt for support and helpful discussions.

Supplementary Materials

www.sciencemag.org/cgi/content/full/337/6098/1075/DC1
Materials and Methods
Supplementary Text
Figs. S1 to S12
Tables S1 to S9
References (35–106)

12 April 2012; accepted 23 July 2012
10.1126/science.1223264

Radiative Absorption Enhancements Due to the Mixing State of Atmospheric Black Carbon

Christopher D. Cappa,^{1*} Timothy B. Onasch,^{2,3*} Paola Massoli,² Douglas R. Worsnop,^{2,4} Timothy S. Bates,⁵ Eben S. Cross,^{3†} Paul Davidovits,³ Jani Hakala,⁴ Katherine L. Hayden,⁶ B. Tom Jobson,⁷ Kathryn R. Kolesar,¹ Daniel A. Lack,^{8,9} Brian M. Lerner,^{8,9} Shao-Meng Li,⁶ Daniel Mellon,^{1‡} Ibraheem Nuaaman,^{6,10} Jason S. Olfert,¹¹ Tuukka Petäjä,⁴ Patricia K. Quinn,⁵ Chen Song,¹² R. Subramanian,¹³ Eric J. Williams,⁸ Rahul A. Zaveri¹²

Atmospheric black carbon (BC) warms Earth's climate, and its reduction has been targeted for near-term climate change mitigation. Models that include forcing by BC assume internal mixing with non-BC aerosol components that enhance BC absorption, often by a factor of ~2; such model estimates have yet to be clearly validated through atmospheric observations. Here, direct in situ measurements of BC absorption enhancements (E_{abs}) and mixing state are reported for two California regions. The observed E_{abs} is small—6% on average at 532 nm—and increases weakly with photochemical aging. The E_{abs} is less than predicted from observationally constrained theoretical calculations, suggesting that many climate models may overestimate warming by BC. These ambient observations stand in contrast to laboratory measurements that show substantial E_{abs} for BC are possible.

Black carbon (BC) in the atmosphere has a strong effect on global and regional climate, with some estimates suggesting that the positive (warming) radiative forcing by BC is second only to CO₂ (1), making it an important near-term climate mitigation target (2, 3). Quantification of the warming caused by BC in global climate models depends explicitly on the mixing state assumed for particles (internal versus external) and, for internal mixtures, the assumed influence of coatings on the magnitude of BC absorption (4–6). Optical properties of internally mixed BC-containing particles can be calculated in various ways, all of which indicate substantially greater absorption than for an equivalent exter-

nal mixture—the absorption by internally mixed BC is “enhanced” because the coatings act as a lens (7). Model estimates of BC radiative forcing are increased by up to a factor of 2 for internally versus externally mixed BC (4, 5), and many models that use external mixtures simply multiply BC absorption by a scaling factor (8) to account for the theoretical absorption enhancement (E_{abs}). However, the magnitude of E_{abs} has not been determined for real atmospheric particles (9, 10), which is crucial as more models describe aerosol distributions as combinations of internal and external mixtures (11).

In this study, direct measurements of E_{abs} and average mixing state for BC in the atmo-

sphere around California are reported from two field campaigns: the 2010 CalNex study and the Carbonaceous Aerosols and Radiative Effects Study (CARES). The CalNex measurements were made onboard the R/V *Atlantis*, whereas the CARES measurements were made at a ground site in the Sacramento urban area (fig. S1) (12). Our observations indicate that the E_{abs} for ambient particles around large urban centers do not vary much with photochemical aging, are significantly less than predicted from traditional core-shell Mie theory, and are in contrast to laboratory experiments, suggesting that the warming by BC may be overestimated in climate models. Further, they indicate a role for absorption by non-BC aerosol components [brown carbon (BrC)] (13) in urban environments at short visible wavelengths.

¹Department of Civil and Environmental Engineering, University of California, Davis, CA 95616, USA. ²Aerodyne Research, Billerica, MA 01821, USA. ³Department of Chemistry, Boston College, Boston, MA 02467, USA. ⁴Department of Physics, University of Helsinki, Helsinki FI-00014, Finland. ⁵National Oceanic and Atmospheric Administration (NOAA) Pacific Marine Environmental Laboratory, Seattle, WA 98115, USA. ⁶Air Quality Research Division, Environment Canada, Toronto M3H 5T4, Canada. ⁷Department of Civil and Environmental Engineering, Washington State University, Pullman, WA 99164, USA. ⁸NOAA Earth System Research Laboratory, Boulder, CO 80305, USA. ⁹Cooperative Institute for Research in Environmental Sciences, University of Colorado, Boulder, CO 80309, USA. ¹⁰Centre for Atmospheric Chemistry, York University, Toronto M3J 1P3, Canada. ¹¹Department of Mechanical Engineering, University of Alberta, Edmonton T6G 2R3, Canada. ¹²Atmospheric Sciences and Global Change Division, Pacific Northwest National Laboratory, Richland, WA 99354, USA. ¹³RTI International, Research Triangle Park, NC 27709, USA.

*To whom correspondence should be addressed. E-mail: cdcappa@ucdavis.edu (C.D.C.); onasch@aerodyne.com (T.B.O.)
†Present address: Massachusetts Institute of Technology, Cambridge, MA 02139, USA.
‡Present address: PCME, St. Ives PE27 3GH, UK.

Photochemical aging of urban air masses leads to the production of nonrefractory particulate matter (NR-PM), some of which is internally mixed with BC and can, in principle, lead to $E_{\text{abs}} > 1$. The fraction of NR-PM exclusively associated with BC is termed here NR-PM_{BC}. The extent to which BC can theoretically be enhanced via lensing depends critically on the ratio $R_{\text{BC}} = [\text{NR-PM}_{\text{BC}}]/[\text{BC}]$ (7). During CalNex, chemically resolved mass concentrations of sub-micrometer NR-PM_{BC} were explicitly measured with a SP-AMS (soot particle–aerosol mass spectrometer) (14), from which R_{BC} is directly quantified. The observed R_{BC} increases rapidly with photochemical age (PCA), which was estimated from the quantity $-\log([\text{NO}_x]/[\text{NO}_y])$ (Fig. 1A). [The ratio $-\log([\text{NO}_x]/[\text{NO}_y])$ serves as a photochemical “clock” by assuming that the conversion of NO_x ($=\text{NO} + \text{NO}_2$) to NO_y occurs at a rate equal to the $\text{NO}_2 + \text{OH}$ reaction rate (12).] This indicates that photochemical aging led to significant pro-

duction of NR-PM_{BC} material and growth of BC-containing particles, in particular through condensation of oxygenated organic aerosol (OOA) and SO_4^{2-} (Fig. 1, B to D, and figs. S8 and S9). These measurements show explicitly how the composition of only the BC-containing particles changes during photochemical aging, providing strong constraints for use in comparing the observed E_{abs} with theoretical calculations.

During CalNex and CARES, E_{abs} was measured as the ratio between ambient particle absorption ($b_{\text{abs,ambient}}$) and the absorption after particle heating in a thermodenuder ($b_{\text{abs,TD}}$) to evaporate and remove non-BC NR-PM, including NR-PM_{BC} (fig. S4) (12). The absorption measurements were made at 532 and 405 nm by using photoacoustic spectroscopy (fig. S3) (12). The observed E_{abs} include effects of both lensing and of BrC absorption (15).

Despite the substantial photochemical production of NR-PM and NR-PM_{BC} and the growth

of BC-containing particles (Fig. 1), the observed E_{abs} values during both campaigns change only slowly with PCA and are not much above unity (Fig. 2). Further, the E_{abs} during CalNex exhibited minimal dependence on R_{BC} (Fig. 3). The average $E_{\text{abs,532nm}}$ during both campaigns is 1.06 ± 0.006 (2 SEM), suggesting that NR-PM_{BC} increased the absorption by 6% on average. The slightly larger E_{abs} at 405 nm [1.13 ± 0.01 (2 SEM)] likely indicates the influence of BrC on absorption in this wavelength region. Consideration of the BC mass absorption coefficient ($\text{MAC}_{\text{BC}} = b_{\text{abs}}/[\text{BC}]$), variations in which have traditionally been used to infer E_{abs} , leads to similar conclusions (although with greater uncertainties) (fig. S17) (12). Overall, these results lead to the unexpected conclusion that photochemical aging and NR-PM_{BC} production did not cause a substantial increase in the absorption enhancement for BC. Single-particle microscopy measurements from locations around the world (16–18) indicate it is common to find BC inclusions at the edge of collected particles rather than deeply embedded in a “coating” material (which would be necessary to observe large absorption enhancements), which is consistent with our ambient observations.

Climate models that account for internal mixing of BC commonly use core-shell Mie theory to calculate the optical properties of BC-containing particles. Time-series of E_{abs} during CalNex have therefore been calculated here by using core-shell Mie theory and binned according to PCA. One feature of our study is that all inputs to the calculations, in particular the particle mixing state (the R_{BC} and size distributions of both BC and non-BC containing particles), were observationally constrained by the comprehensive suite of instrumentation available during CalNex (12). E_{abs} was calculated for either a unimodal or bimodal distribution of coating thicknesses on the BC particles (fig. S7) (12). The calculated E_{abs} are significantly greater than the observed values at all PCAs, demonstrating that core-shell Mie theory substantially overestimates the actual E_{abs} , even when explicitly constrained by observations of R_{BC} (Fig. 2). The difference between the bimodal and unimodal simulations illustrates the importance of mixing state assumptions to the calculations. If all NR-PM (not just NR-PM_{BC}) had been assumed to be internally mixed with BC, the overprediction of E_{abs} would have been even larger because only ~20% of the total sub-micrometer NR-PM was NR-PM_{BC}, on average. This is an important consideration for models that assume internal mixing but do not dynamically account for the distribution of NR-PM between BC and non-BC-containing particles.

These ambient observations are in contrast to results from laboratory experiments we conducted in which large $E_{\text{abs,532nm}}$ values were observed when flame-generated BC was internally mixed with dioctyl sebacate (DOS) (Fig. 3) (12). For a given BC particle size, the measured E_{abs} increased with R_{BC} (which varied over the same range as the ambient R_{BC}) and were generally consistent with

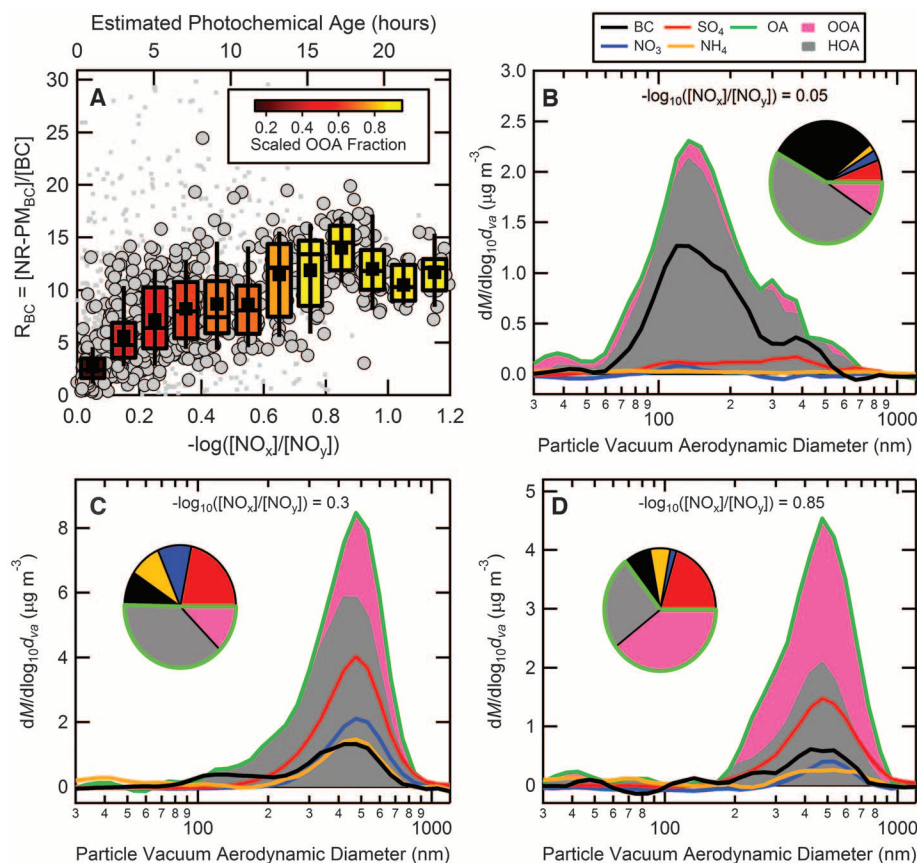


Fig. 1. (A) The $R_{\text{BC}} (= [\text{NR-PM}_{\text{BC}}]/[\text{BC}])$ ratio as a function of PCA ($-\log([\text{NO}_x]/[\text{NO}_y])$) for total NR-PM_{BC} during CalNex. The box and whisker plots show the mean (■), median (—), lower and upper quartile (boxes), and 9th and 91st percentile (whisker) results for periods in which $[\text{BC}] > 0.07 \mu\text{g m}^{-3}$ (light gray points, ●). For reference, the gray dots show all data. The corresponding PCA (assuming $[\text{OH}] = 4 \times 10^6 \text{ molecules cm}^{-3}$) is shown on the top axis. The boxes are color-coded according to the scaled oxygenated organic aerosol (OOA) fraction of total OA (12). (B to D) Chemically resolved mass-weighted particle time-of-flight vacuum aerodynamic diameter (d_{va}) size distributions from the SP-AMS for BC internally mixed with NR-PM_{BC}, including SO_4^{2-} , NO_3^- , NH_4^+ , and OA, for periods where $-\log([\text{NO}_x]/[\text{NO}_y])$ was (B) 0.05 (fresh; $R_{\text{BC}} = 3.1$), (C) 0.3 (intermediate; $R_{\text{BC}} = 10.3$), and (D) 0.85 (aged; $R_{\text{BC}} = 15.8$). The total OA has been split into two OA types identified from factor analysis as hydrocarbon-like organic aerosol (HOA) and OOA. The pie charts show the fractional contributions of the various species to the total mass of BC-containing particles.

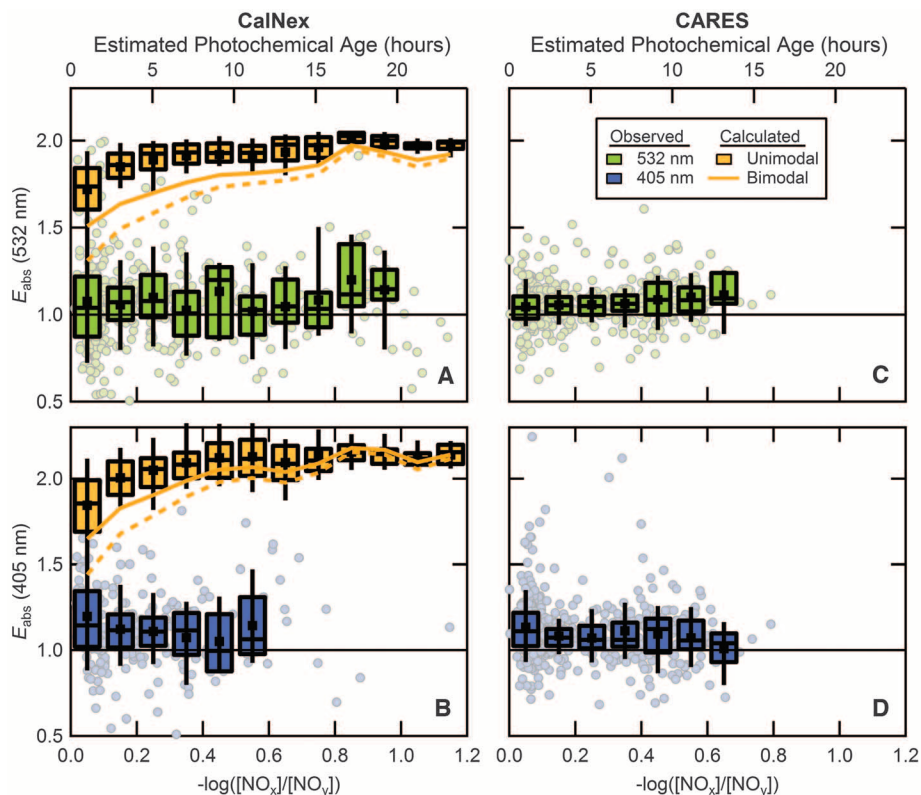
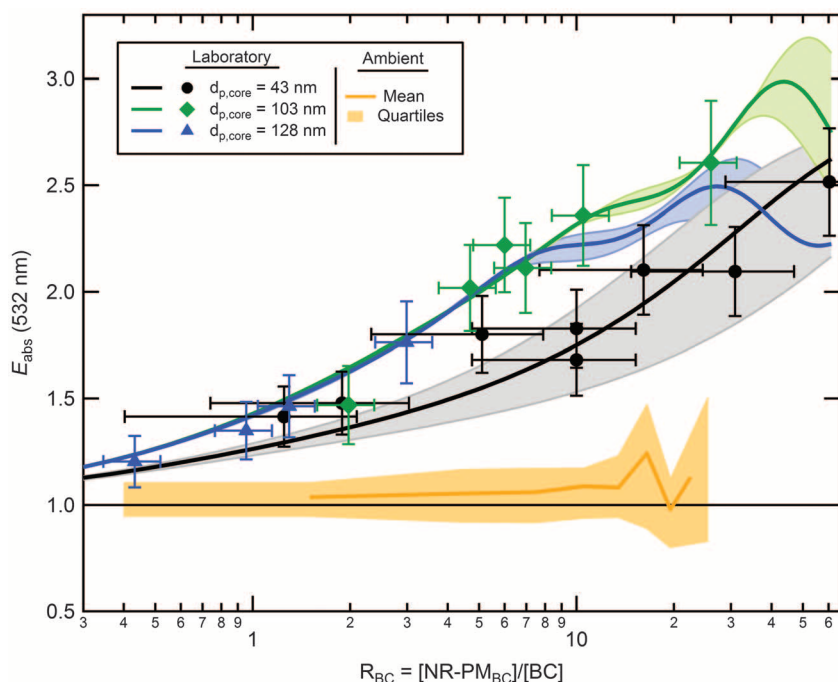


Fig. 2. Measured E_{abs} at (A and C) 532 nm (green) and (B and D) 405 nm (blue) for CalNex [(A) and (B)] and CARES [(C) and (D)] as a function of PCA, estimated from $-\log([\text{NO}_x]/[\text{NO}_y])$. The light-colored points correspond to individual measurements, whereas the box and whisker plots show the binned mean (\blacksquare), median ($-$), lower and upper quartile (boxes), and 9th and 91st percentile (whisker). Calculated E_{abs} values for CalNex are shown, assuming that the distribution of NR-PM_{BC} material on the BC-containing particles was either bimodal (orange lines) or unimodal (orange box and whisker). For the bimodal case, one mode was assumed to be “thickly” coated, whereas the other was “thinly” coated. The thinly coated mode was assumed to have either $R_{\text{BC}} = 1$ (solid) or 0.1 (dashed).

Fig. 3. Observed E_{abs} at 532 nm as a function of R_{BC} for laboratory experiments in which BC particles of various size, produced from ethylene flame, were coated with dioctyl sebacate (symbols). The $d_{\text{p,core}}$ values are the volume-equivalent diameter of the uncoated BC particles. Uncertainties are 1σ . Calculated E_{abs} from core-shell Mie theory (lines) are shown for the differently sized BC particles and are in generally good agreement with the observations; the colored bands show the uncertainty range in the calculations. The observed mean ambient particle E_{abs} versus R_{BC} during CalNex is shown for comparison (orange line).



core-shell theory. These laboratory results clearly demonstrate that internal mixing of BC with NR-PM can produce large E_{abs} , as has previously been observed (19, 20). Further work is needed to resolve the discrepancies between field observations and laboratory studies.

Although there is no evidence of strong lensing-induced absorption enhancements at 532 nm, the slightly larger E_{abs} at 405 nm suggests absorption by some NR-PM species at shorter wavelengths occurred; we assume the absorbing NR-PM species to be BrC. BrC is particulate organic carbon that absorbs light at visible and near-ultraviolet (UV) wavelengths (13), with the absorption increasing strongly toward shorter wavelengths (21). Here, the difference between $E_{\text{abs},405\text{nm}}$ and $E_{\text{abs},532\text{nm}}$ can be interpreted as the approximate contribution to absorption by BrC at 405 nm—whether it exists internally mixed with BC or not (15). For both CalNex and CARES, BrC absorption is $\sim 10\%$ of the total absorption at 405 nm (Fig. 2), corresponding to campaign average MACs for BrC of $0.12 \text{ m}^2/\text{g}$ (CalNex) and $0.14 \text{ m}^2/\text{g}$ (CARES) and a derived imaginary refractive index of ~ 0.004 (12). This additional absorption by NR-PM in the near-UV region can have an impact on photochemical O_3 production (22, 23) and could suppress OH concentrations, thus increasing the lifetime of greenhouse gases such as methane or affecting the conversion of SO_2 into scattering sulfate aerosol (24).

Our measurements indicate that BC emitted from large to medium-sized urban centers (dominated by fossil fuel emissions) does not exhibit a substantial absorption enhancement when internally mixed with non-BC material, which is in stark contrast to laboratory experiments and model calculations. The small observed values

of E_{abs} suggest that models that assume internal mixtures in a core-shell configuration, or scale the absorption (or forcing) by externally mixed BC particles, can substantially overestimate the atmospheric warming by BC, potentially by up to a factor of 2 (4, 5). The climate benefits of BC mitigation (3) would similarly be overestimated. This would be true even for models that specifically track the mixing state of BC particles as they evolve in time (25). It is possible that non-fossil-derived BC (such as emitted from biomass burning) may exist with a considerably different internal morphology or amounts of BrC as compared with the ambient particles observed in this study, and thus different observable E_{abs} values. Models may ultimately need to treat BC from fossil-fuel combustion differently than BC from biomass burning, although this awaits validation through further measurements of wavelength-dependent E_{abs} for atmospheric particles in a variety of locations around the world. The contrast between our ambient observations and model formulations highlights the still incomplete understanding of radiative forcing by atmospheric BC with respect to particle-mixing state. Additional challenges include the quantification of BC emission inventories, wet-deposition removal rates,

and the specification of the spatial and temporal distributions of BC (particularly the altitudinal profile) (26).

References and Notes

- V. Ramanathan, G. Carmichael, *Nat. Geosci.* **1**, 221 (2008).
- A. P. Grieshop, C. C. O. Reynolds, M. Kandlikar, H. Dowlatabadi, *Nat. Geosci.* **2**, 533 (2009).
- D. Shindell *et al.*, *Science* **335**, 183 (2012).
- S. H. Chung, J. H. Seinfeld, *J. Geophys. Res.* **110**, (D11), D11102 (2005).
- M. Z. Jacobson, *Nature* **409**, 695 (2001).
- G. Myhre, *Science* **325**, 187 (2009).
- T. C. Bond, G. Habib, R. W. Bergstrom, *J. Geophys. Res.* **111**, (D20), D20211 (2006).
- J. Hansen *et al.*, *Clim. Dyn.* **29**, 661 (2007).
- A. Knox *et al.*, *Aerosol Sci. Technol.* **43**, 522 (2009).
- C. Doran, *Atmos. Chem. Phys.* **7**, 2197 (2007).
- S. J. Ghan, S. E. Schwartz, *Bull. Am. Meteorol. Soc.* **88**, 1059 (2007).
- Materials and methods are available as supplementary materials on Science Online.
- M. O. Andreae, A. Gelencser, *Atmos. Chem. Phys.* **6**, 3131 (2006).
- T. B. Onasch *et al.*, *Aerosol Sci. Technol.* **46**, 804 (2012).
- D. A. Lack, C. D. Cappa, *Atmos. Chem. Phys.* **10**, 4207 (2010).
- K. Adachi, S. H. Chung, P. R. Buseck, *J. Geophys. Res.* **115**, (D15), D15206 (2010).
- K. S. Johnson *et al.*, *Atmos. Chem. Phys.* **5**, 3033 (2005).
- J. Li, J. R. Anderson, P. R. Buseck, *J. Geophys. Res.* **108**, (D6), 4189 (2003).

- E. S. Cross *et al.*, *Aerosol Sci. Technol.* **44**, 592 (2010).
- M. Schnaiter *et al.*, *J. Geophys. Res.* **110**, (D19), D19204 (2005).
- J. C. Barnard, R. Volkamer, E. I. Kassianov, *Atmos. Chem. Phys.* **8**, 6665 (2008).
- R. R. Dickerson *et al.*, *Science* **278**, 827 (1997).
- M. Z. Jacobson, *J. Geophys. Res.* **104**, (D3), 3527 (1999).
- D. T. Shindell *et al.*, *Science* **326**, 716 (2009).
- R. A. Zaveri, J. C. Barnard, R. C. Easter, N. Riemer, M. West, *J. Geophys. Res.* **115**, (D17), D17210 (2010).
- D. Koch *et al.*, *Atmos. Chem. Phys.* **9**, 9001 (2009).

Acknowledgments: The authors thank the crew of the R/V *Atlantis*, the support at American River College and Combustion for loan of the centrifugal particle mass analyzer (CPMA). This work was supported by the NOAA Climate Program Office (NA09OAR4310124 and NA09OAR4310125), U.S. Environmental Protection Agency (RD834558), NSF Atmospheric Chemistry, California Air Resources Board, U.S. Department of Energy (DOE) Atmospheric System Research (ASR) program and DOE Atmospheric Radiation Measurement (ARM) Climate Research Facility, the Canadian Federal Government (PERD Project C12.007), and the Natural Sciences and Engineering Research Council of Canada.

Supplementary Materials

www.sciencemag.org/cgi/content/full/337/6098/1078/DC1

Materials and Methods

Figs. S1 to S19

References

17 April 2012; accepted 3 July 2012

10.1126/science.1223447

A Gain-of-Function Polymorphism Controlling Complex Traits and Fitness in Nature

Kasavajhala V. S. K. Prasad,^{1*} Bao-Hua Song,^{1*} Carrie Olson-Manning,^{1*} Jill T. Anderson,¹ Cheng-Ruei Lee,¹ M. Eric Schranz,^{1†} Aaron J. Windsor,^{1‡} Maria J. Clauss,² Antonio J. Manzaneda,^{1§} Ibtehaj Naqvi,^{1||} Michael Reichelt,² Jonathan Gershenzon,² Sanjeewa G. Rupasinghe,^{3¶} Mary A. Schuler,³ Thomas Mitchell-Olds^{1#}

Identification of the causal genes that control complex trait variation remains challenging, limiting our appreciation of the evolutionary processes that influence polymorphisms in nature. We cloned a quantitative trait locus that controls plant defensive chemistry, damage by insect herbivores, survival, and reproduction in the natural environments where this polymorphism evolved. These ecological effects are driven by duplications in the *BCMA* (branched-chain methionine allocation) loci controlling this variation and by two selectively favored amino acid changes in the glucosinolate-biosynthetic cytochrome P450 proteins that they encode. These changes cause a gain of novel enzyme function, modulated by allelic differences in catalytic rate and gene copy number. Ecological interactions in diverse environments likely contribute to the widespread polymorphism of this biochemical function.

Few studies have identified the genes that underlie complex trait variation in nature and the evolutionary processes that influence these polymorphisms. Most such work has focused on loss-of-function mutations that lead to adaptive phenotypes (1), likely because novel gain-of-function changes occur infrequently and require persistent natural selection to be maintained in populations (2). Nonetheless, new functional mechanisms are crucially important for adaptive evolution (3). To understand the adaptive consequences of complex trait variation, we

must establish a direct relationship between genetic polymorphisms and phenotypic traits, and investigate the fitness consequences of this variation in natural environments (1).

Glucosinolates are biologically active secondary compounds (fig. S1) found in *Arabidopsis* and its relatives (4) that are important in many aspects of plant defense, influencing oviposition and feeding by insect herbivores (5), defense against microbial pathogens (6), and composition of associated microbial communities (7). Typically, generalist insects are sensitive to glucosinolate-

based plant defenses, whereas specialists may be able to cope with these compounds, which may serve as oviposition cues and feeding stimulants (5).

The ecological model plant *Boechera stricta* (Brassicaceae) is a native, short-lived perennial with a close phylogenetic relationship to *Arabidopsis* (8), often found in undisturbed habitats where current environments are similar to historical conditions that have existed for ~3000 years (9). In field populations near Lost Trail Pass in Montana and Crested Butte in Colorado, we measured natural selection on foliar damage from herbivores using local genotypes. We mapped a quantitative trait locus (QTL) in *B. stricta* that contributes to insect resistance and controls allocation to glucosinolates derived from branched-chain amino acids or methionine [the *BCMA* (branched-chain methionine allocation) locus] (10). Although most Brassicaceae synthesize glucosinolates from

¹Department of Biology, Institute for Genome Sciences and Policy, Duke University, Durham, NC 27708, USA. ²Max Planck Institute for Chemical Ecology, D-07745 Jena, Germany. ³Department of Cell and Developmental Biology, University of Illinois at Urbana-Champaign, Urbana, IL 61801, USA.

*These authors contributed equally to this work.

†Present address: Biosystematics Group, Wageningen University, 6708 PB Wageningen, Netherlands.

‡Present address: Bayer CropScience N.V., 9052 Ghent, Belgium.

§Present address: Departamento de Biología Animal, Biología Vegetal y Ecología, Área de Ecología, Universidad de Jaén, 23071 Jaén, Spain.

||Present address: Duke University School of Medicine, Durham, NC 27710, USA.

¶Present address: Pfizer Inc., MS 8118A-2053, Eastern Point Road, Groton, CT 06340, USA.

#To whom correspondence should be addressed. E-mail: tmo1@duke.edu